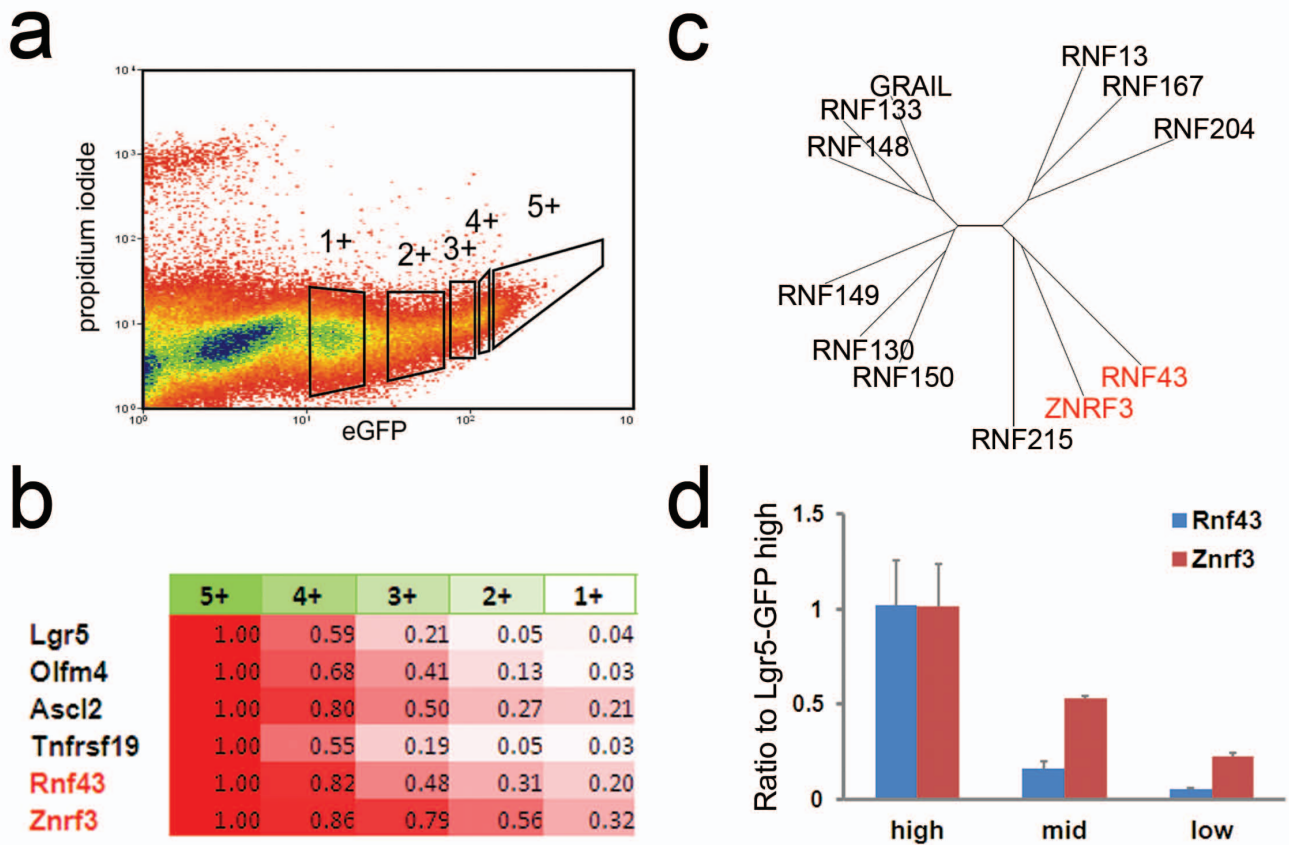
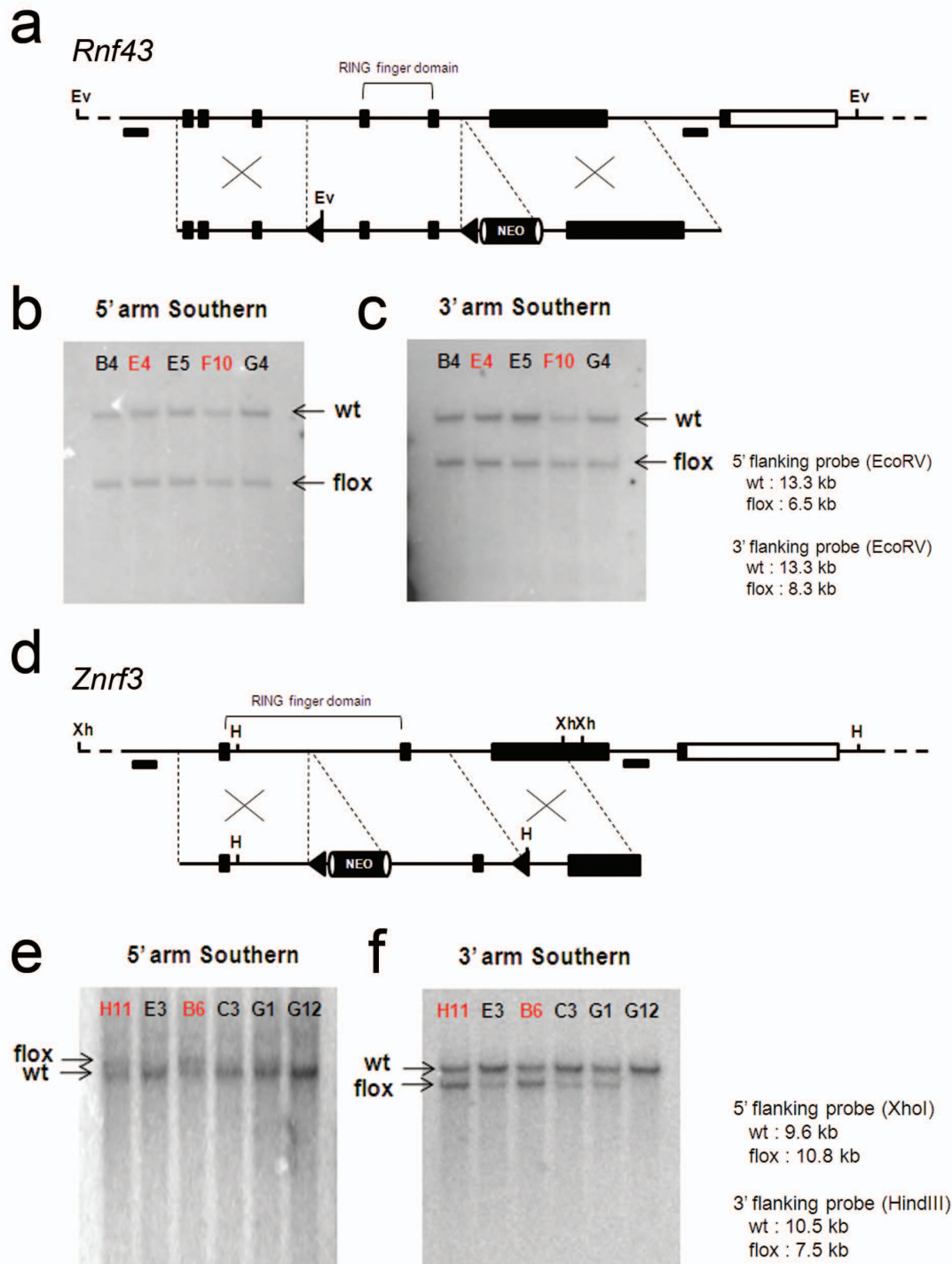


HCT116 cell line: β -catenin 1 wt, 1 mutant allele (constitutively active). RNF43 both alleles have frame shift mutation.

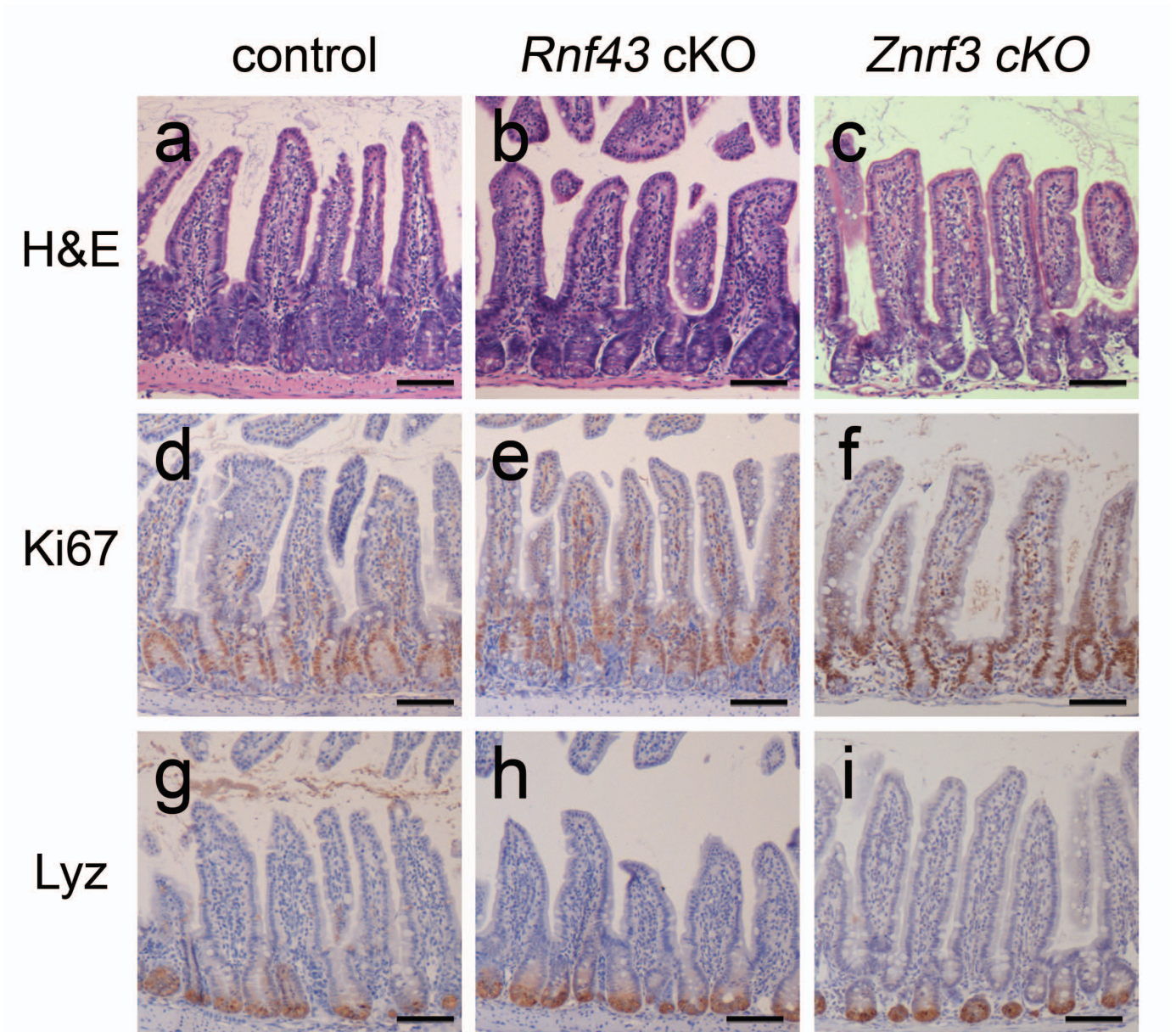
Supplementary Figure 1 | Model of negative feedback regulation of the Wnt pathway by RNF43 and ZNRF3. **a**, Left, in the resting stage, the destruction complex degrades cytosolic β -catenin thereby preventing downstream gene activation. Middle, upon Wnt stimulation, Frizzled and LRP5/6 receptors bind and inactivate the destruction complex, which leads to the accumulation of β -catenin and its migration to the nucleus. The formation of a nuclear TCF/ β -catenin complex induces gene expression of RNF43 and ZNRF3. Right, the transmembrane E3 ligases RNF43 and ZNRF3 ubiquitinate Frizzled at the plasma membrane and, consequently, promote its endocytosis and lysosomal degradation. The decrease of Frizzled receptors at the cell surface renders the cell insensitive to Wnt stimulation. **b**, Left, HCT116 cells carry one wild-type allele and one mutated, constitutively active allele of β -catenin, while expression of both RNF43 alleles is lost due to frame shift mutations. The active form of β -catenin sustains a basal level of Wnt activation in HCT116 cells. Middle, upon Wnt stimulation, significantly enhanced levels of Wnt activation are achieved due to the lack of negative feedback mediated by RNF43. Right, ectopic expression of RNF43 in HCT116 results in low level of Wnt activation.



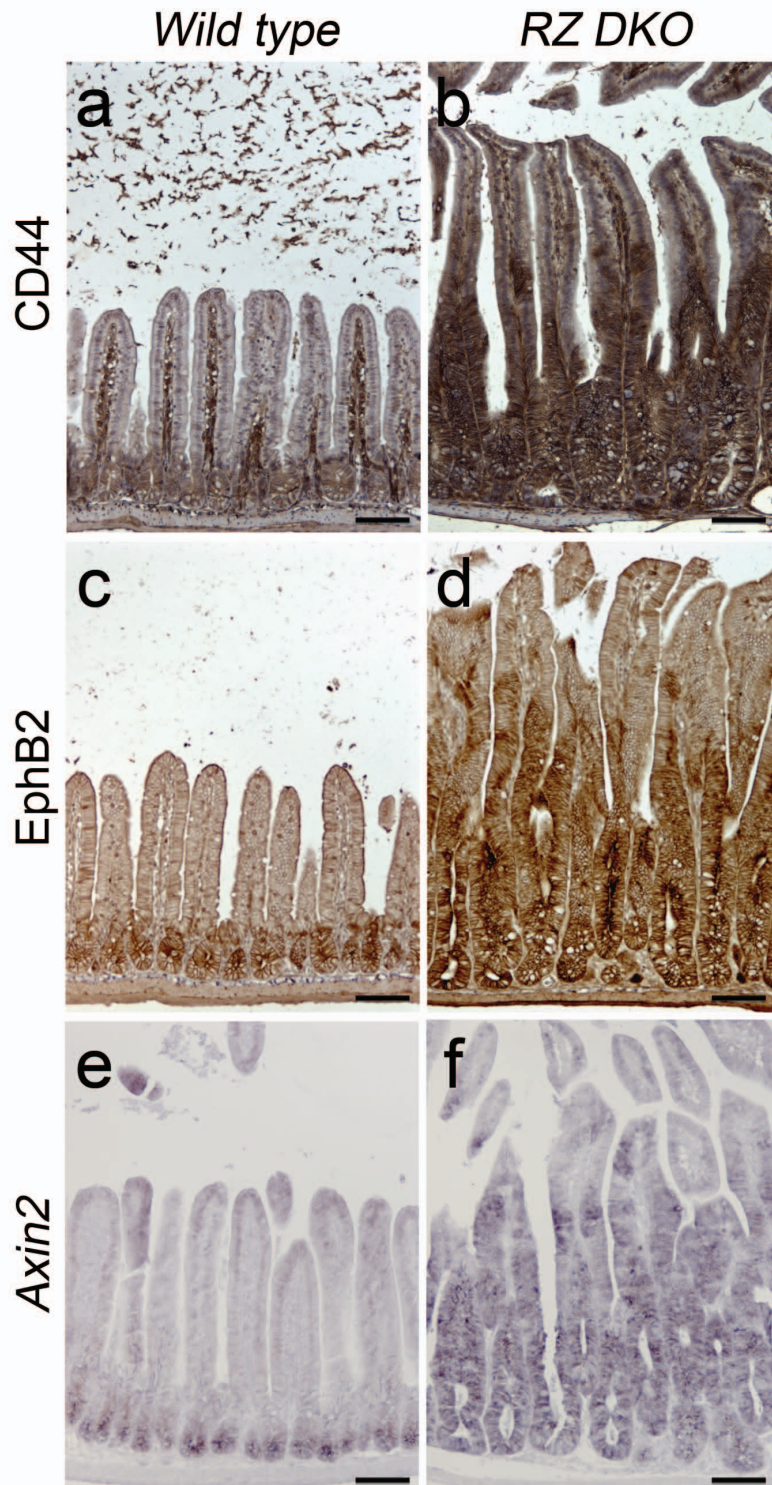
Supplementary Figure 2 | Intestinal Lgr5 stem cell-specific expression of *Rnf43* and *Znrf3*. **a**, Dot plot of flow cytometric analysis indicating the gates for each fraction of Lgr5-GFP-positive cells. Each fraction is labelled from GFP-highest (5+) to GFP-lowest (1+). Propidium iodide is used to exclude dead cells. **b**, Summary of the expression pattern of stem cell genes (*Lgr5*, *Olfm4*, *Ascl2* and *Tnfrsf19*) and two RING-type E3 ubiquitin ligases (*Rnf43* and *Znrf3*). Every fraction is compared to fraction 5+. Note that the expression levels of *Rnf43* and *Znrf3* follow the expression pattern of other stem cell genes. **c**, Phylogenetic tree of 12 PA-TM-RING (PA, PA domain; TM, transmembrane; RING, RING domain) proteins in human. RNF43 and ZNRF3 are two closely related paralogues among the 12 members. **d**, Quantitative RT-PCR for *Rnf43* and *Znrf3*. Based on the intensity of GFP expression, Lgr5-GFP high, middle (mid) and low cells were isolated. Error bar: s.d., n=3. Three technical replicates for the quantitative RT-PCR result (d).



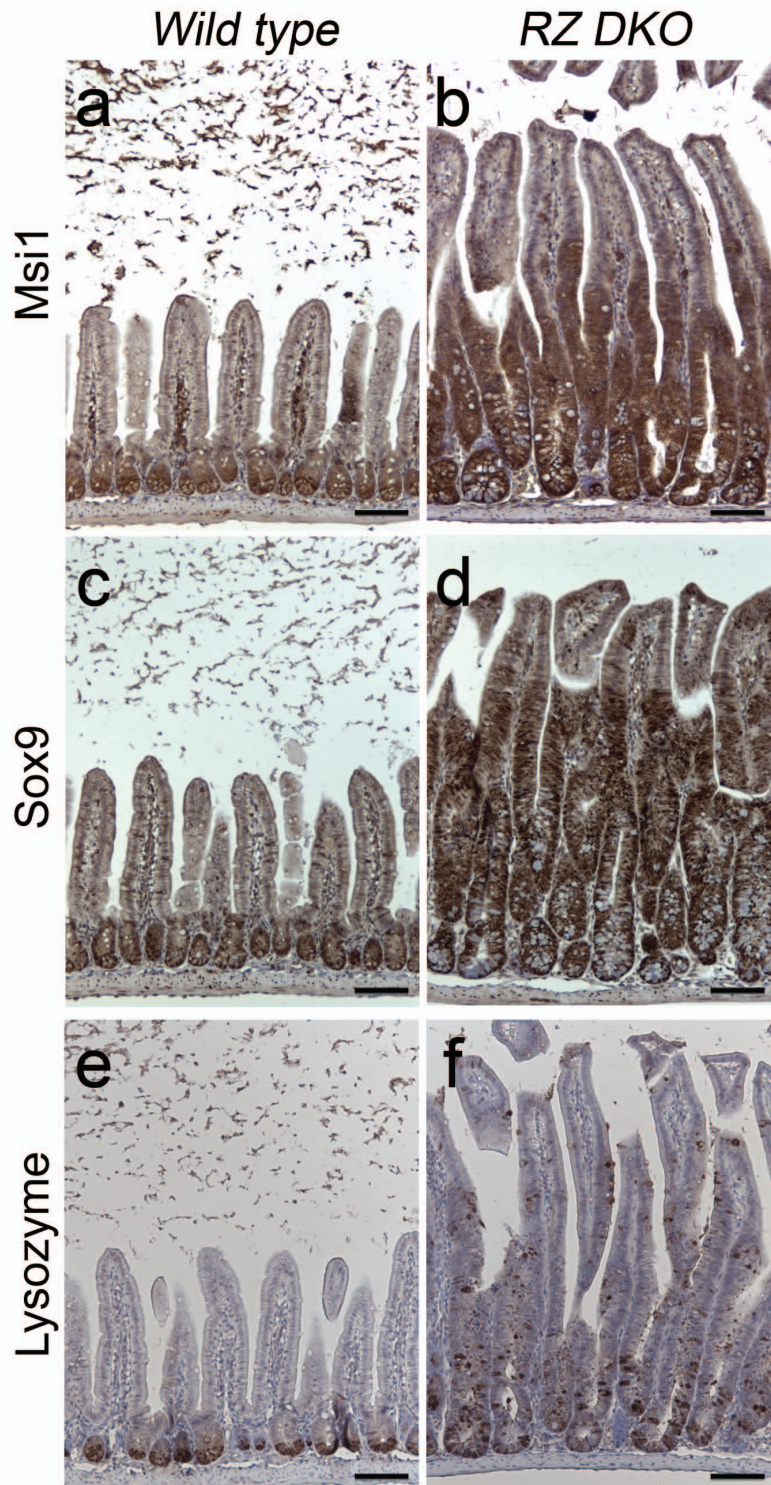
Supplementary Figure 3| Targeting strategy of *Rnf43* and *Znrf3*. **a**, Schematic overview of the *Rnf43* targeting strategy. Two exons encoding the RING domain of *Rnf43* are flanked by LoxP sites. **b**, **c**. Southern blot analysis of targeted clones with 5' flanking probe (**b**) and 3' flanking probe (**c**). The restriction enzyme used for the analysis and the expected size of the bands are indicated. **d**, Schematic overview of the *Znrf3* targeting strategy. One of the two exons encoding the RING domain of *Znrf3* is flanked by LoxP sites. **e**, **f**. Southern blot analysis of targeted clones with 5' flanking probe (**e**) and 3' flanking probe (**f**). The restriction enzymes used for the analysis and the expected size of bands are indicated. Clones indicated in red were used to generate chimeric mice to get the *Rnf43* and *Znrf3* conditional alleles.



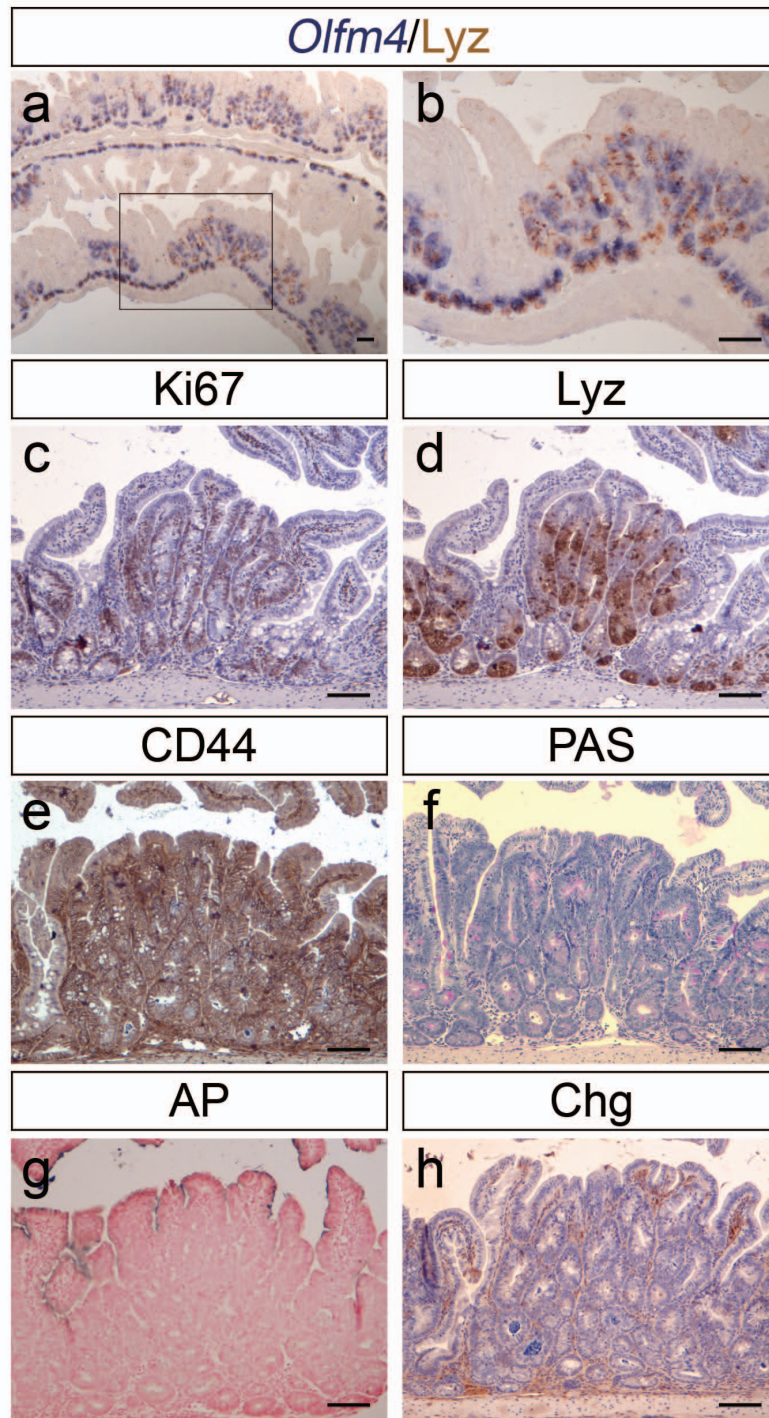
Supplementary Figure 4 | No discernible phenotype of *Rnf43* and *Znrf3* single mutants. a-i, *Wild type* (control; a, d and g), *Rnf43* conditional mutant (*Rnf43* cKO; b, e and h) and *Znrf3* conditional mutant (*Znrf3* cKO; c, f, and i) intestinal sections are stained for H&E (a, b, and c), Ki67 (d, e, and f, for proliferating cells) and Lysozyme (Lyz) (g, h, and i, for Paneth cells). Note that the number of proliferating cells and Paneth cells are comparable between different genotypes. Scale bar: 50 μ m.



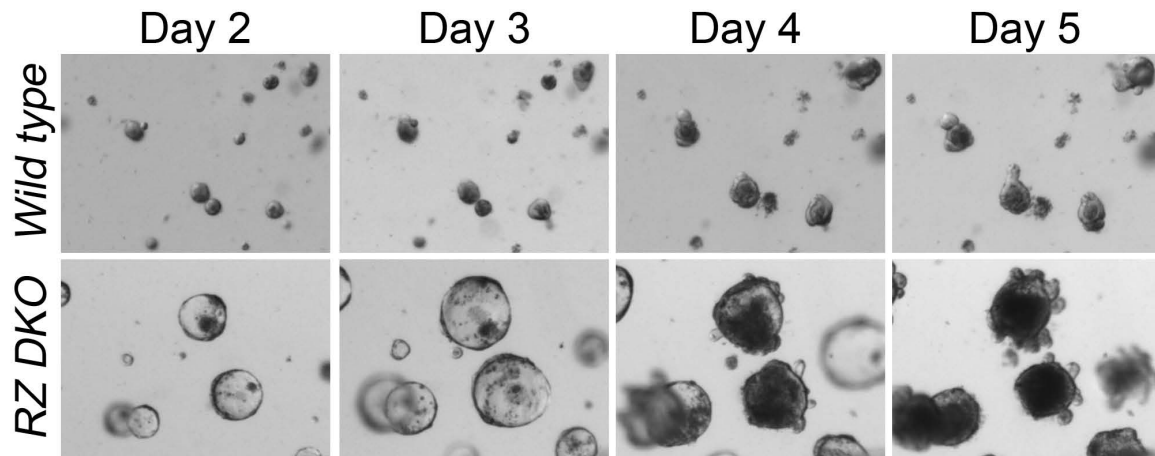
Supplementary Figure 5 | Strong activation of Wnt target gene expression in *Rnf43;Znrf3* compound mutant. a-f, Wild type (a, c and e) and *Rnf43;Znrf3* compound mutant (RZ DKO) (b, d and f) intestinal sections are stained for Wnt-target genes, CD44 (a and b), EphB2 (c and d) and *Axin2* (e and f). Scale bar: 100 μ m.



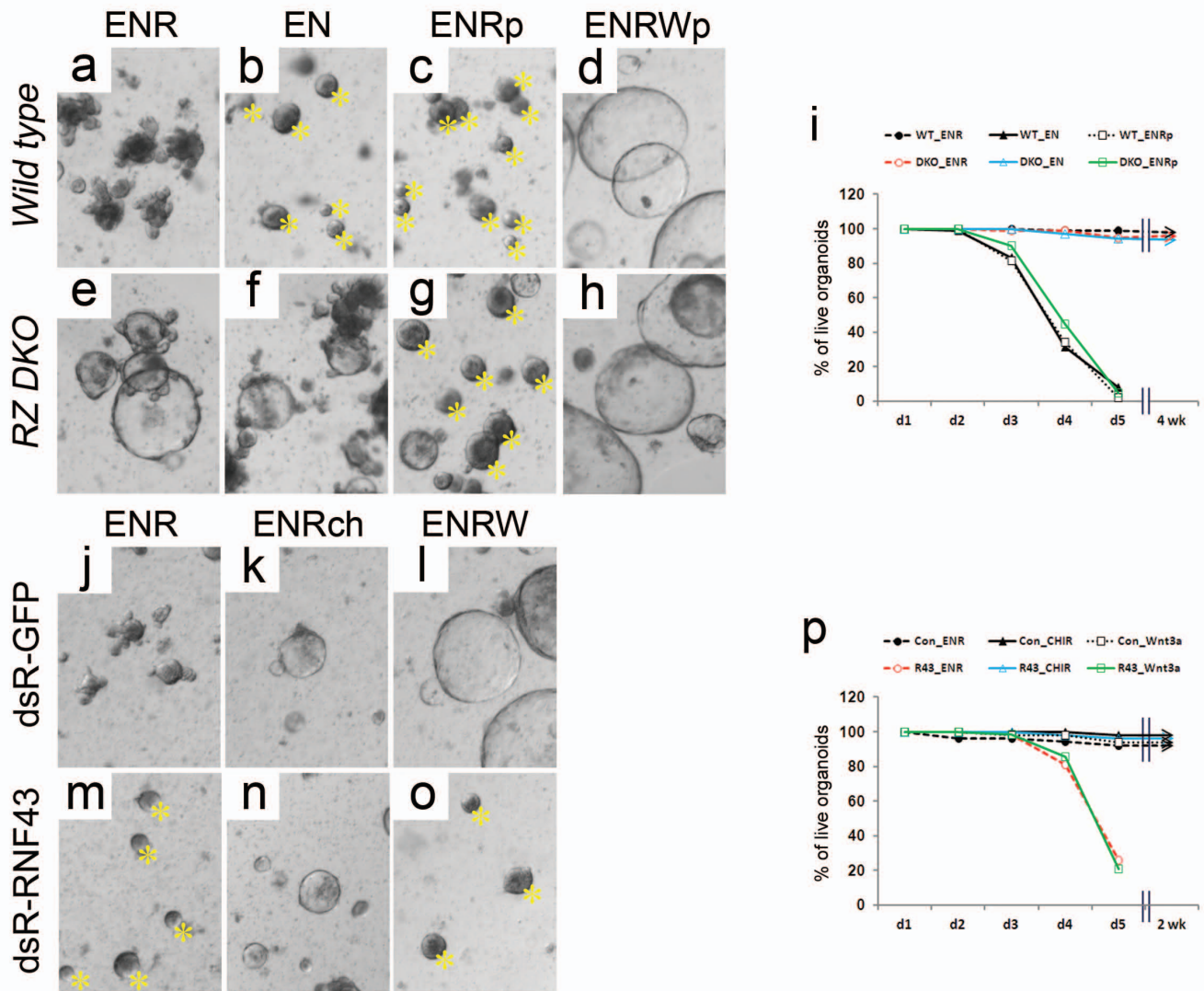
Supplementary Figure 6 | Increased number of progenitors and Paneth cells in *Rnf43;Znrf3* compound mutant. a-f, Wild type (a, c and e) and *Rnf43;Znrf3* compound mutant (*RZ DKO*) (b, d and f) intestinal sections are stained for progenitor cell markers, Msi1 (a and b) and Sox9 (c and d), and the Paneth cell marker, Lysozyme (e and f). Scale bar: 100 μ m.



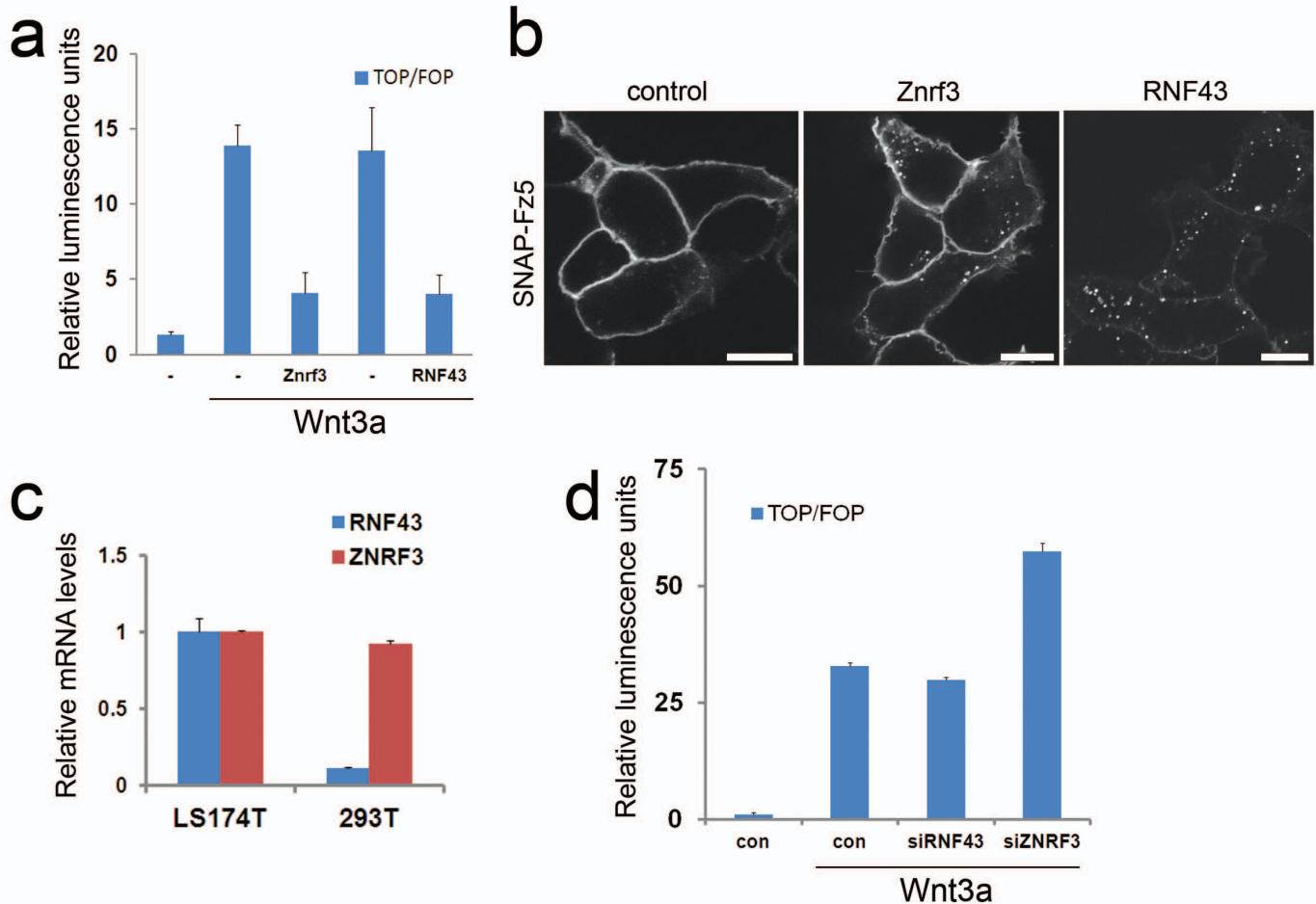
Supplementary Figure 7 | Clonal deletion of *Rnf43* and *Znrf3* in *Lgr5* stem cells results in intestinal polyposis. a-h, Multiple adenomas are formed in *Lgr5-GFPiresCreER;Rnf43;Znrf3* compound mutant intestine after tamoxifen induction. Formation of adenoma was observed one month after tamoxifen treatment. Adenomas are stained for *Olfm4* (blue, for stem cells) and Lysozyme (Lyz, brown, for Paneth cells) (a, b), Ki67 (c, for proliferating cells), Lyz (d, for Paneth cells), CD44 (e, for Wnt-active cells), PAS (f, for goblet cells), Alkaline phosphatase (AP, g, for enterocytes), and Chromogranin (Chg, for enteroendocrine cells). b shows a high magnification image of the rectangled region in a. Note that adenomas mainly consist of proliferating progenitor/stem cells and Paneth cells. Scale bar: 100 μ m.



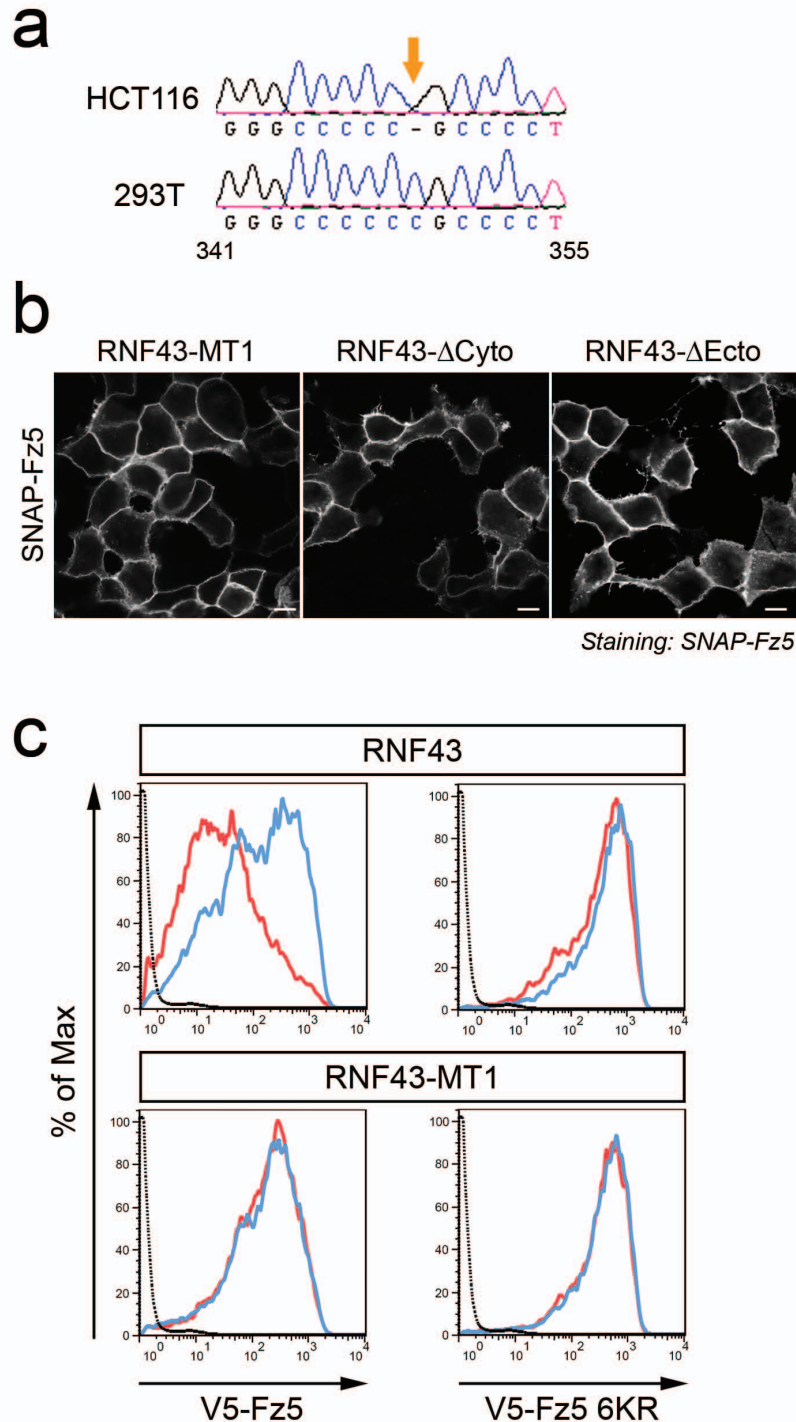
Supplementary Figure 8 | Growth of organoids. *Wild type* and *RZ DKO* organoids under normal growth conditions containing Egf, Noggin and Rspo1. Note that *RZ DKO* organoids grow significantly faster than control organoids.



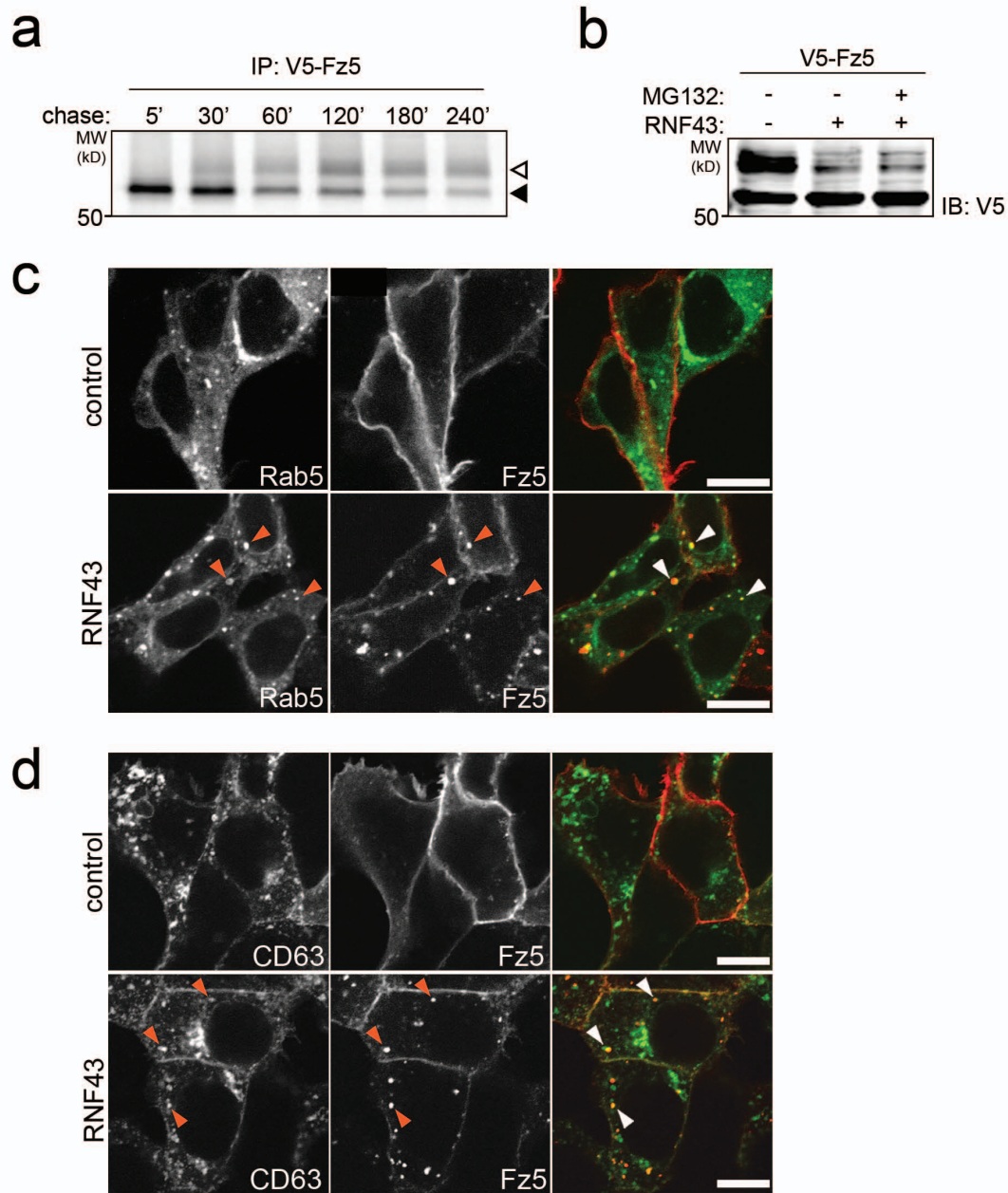
Supplementary Figure 9 | *In vitro* phenotyping using organoids. **a-h**, *Wild type* (a, b, c and d) and *RZ DKO* (e, f, g and h) organoids under various growth conditions (E, Egf; N, Noggin; R, Rspo1; p, porcupine inhibitor (IWP1) and W, Wnt3a). Note that *RZ DKO* organoids grow in the absence of Rspo1. Asterisks indicate dying organoids on day 3 which were confirmed to be dead on day 5. **i**, Survival curve of organoids in each condition. Arrow indicates that organoids in the condition can grow for >4 weeks. **j-o**, DsR-GFP (j, k and l; control) and dsR-RNF43 (m, n and o) overexpressing organoids under various growth conditions (ch, GSK3 β inhibitor (CHIR99021) and W, Wnt3a). Note that RNF43 overexpression-mediated growth arrest is restored by inhibiting GSK3 β . Asterisks indicate dying organoids on day 3 which were confirmed to be dead on day 5. **p**, Survival curve of organoids in each condition. Arrow indicates that organoids in the condition can grow for >2 weeks. The average of two biological replicates is shown (i and p).



Supplementary Figure 10 | Znr3 has a similar function to RNF43. **a**, Luciferase assay of TCF4- β -catenin activity in the presence of Znr3 and RNF43. Both Znr3 and RNF43 abolish Wnt3a-activated luciferase activity in HEK293T cells. **b**, Subcellular localisation of SNAP-Fz5 in the absence or presence of Znr3-HA or RNF43-HA in HEK293T cells. Surface SNAP-Fz5 was labelled with SNAP-Alexa⁵⁴⁹ for 15 minutes and chased for 15 minutes. Scale bars 10 μ m. **c**, Quantitative RT-PCR for *RNF43* and *ZNRF3* in LS174T colon cancer cells and HEK293T cells. **d**, Luciferase assay of TCF4- β -catenin activity upon knockdown of ZNRF3 and RNF43 by esiRNA. Depletion of ZNRF3 in HEK293 cells induces a modest enhancement of Wnt signalling activity. Error bar: s.d., $n=3$. Three independent biological experiments were performed for the luciferase assays (a and d) and three technical replicates for the quantitative RT-PCR result (c).



Supplementary Figure 11| Both RING activity and the ecto-domain of RNF43 are important to promote Fz5 internalisation. **a**, Frame shift mutation in *RNF43* in HCT116 cells. **b**, Subcellular localisation of SNAP-Frizzled-5 (SNAP-Fz5) in HEK293T cells co-transfected with RNF43-mutants (RNF43-MT1, ligase dead point mutant; RNF43- Δ Cyto, deletion of the cytoplasmic portion; RNF43- Δ Ecto, deletion of the extracellular portion) as indicated. Scale bars 10 μ m. **c**, Flowcytometric analysis of HEK293 cells with doxycycline (Dox)-inducible RNF43 and RNF43-MT1 expressing V5-Fz5 and V5-Fz5 6KR. RNF43 decreases surface levels of Fz5. Blue line, Dox (-); Red line, Dox (+); Dotted line, untransfected cells.



Supplementary Figure 12 | RNF43 triggers endocytosis of Fz5. **a**, Complex glycosylated Fz5 is derived of a lower MW immature Fz5 form. HEK293T cells expressing V5-Fz5 were pulse-labeled with [³⁵S]methionine for 15 min and chased for the indicated time-points. Between 30-120 min chase, the mature complex glycosylated form of Fz5 gradually increases, while the immature form decreases over time. Arrowheads: immature (filled) and mature (open) V5-Fz5. **b**, Down regulation of mature V5-Fz5 levels by RNF43 cannot be rescued by proteasomal inhibition. HEK293T cells co-expressing V5-Fz5 and RNF43-HA were treated either with vehicle or the proteasomal inhibitor MG132 (20uM) for 3 hours. **c**, RNF43 targets SNAP-Fz5 to Rab5+ endosomes. Subcellular localisation of SNAP-Fz5 and GFP-Rab5 in HEK293T cells in the absence or presence of RNF43. **d**, RNF43 targets SNAP-Fz5 to CD63+ lysosomes. Subcellular localisation of SNAP-Fz5 and CD63-GFP in HEK293T cells in the absence or presence of RNF43. Surface SNAP-Fz5 was labelled with SNAP-Alexa⁵⁴⁹ for 15 minutes and chased for 5 minutes. Arrowheads indicate co-localisation. Scale bars 10 μ m.